In-situ growth of $YBa_2Cu_3O_y$ superconducting films by reactive coevaporation at low pressure using ozone

H.M. Appelboom, A.W. Fortuin, G. Rietveld, V.C. Matijasevic, P. Hadley, D. van der Marel, and J.E. Mooij.

Department of Applied Physics, TU Delft, P.O. Box 5046, 2600 GA Delft, The Netherlands.

Abstract

$YBa_2Cu_3O_y$ thin films are grown in-situ on $SrTiO_3$ and MgO substrates using MBE techniques and ozone. Yttrium and copper are evaporated from electron guns and barium is evaporated from a Knudsen cell. Pressure and substrate temperature have been varied to study growth conditions. The results are compared to thermodynamic stability conditions for $YBa_2Cu_3O_y$ and oxygen. The use of ozone enables growth of in situ superconducting films at pressures substantially below the $YBa_2Cu_3O_y$ stability line for oxygen. The films are analyzed with R(T) and x-ray diffraction measurements. The best film so far has been grown on $SrTiO_3$ and has a $T_{c,0}$ of 83 K.

1. INTRODUCTION

High temperature superconductor thin films can be made by several fabrication methods, such as sputtering, laser ablation, MOCVD and evaporation techniques. When the superconductor is crystallized during the deposition lower temperatures can be used compared to typical post annealing temperatures. This lower temperature will result in fewer reactions at the superconductor-substrate interface and in less reactions with artificial barriers. Several succesful attempts to fabricate in-situ superconducting thin films at considerably lower growth temperatures as compared to post-annealing processes have been reported by other groups using various techniques[1,2,3,4]. The evaporation method requires the use of multiple sources for the fabrication of $YBa_2Cu_3O_y$ thin films. This enables one to study the dependance of film properties on compostion[5,6] or to grow artificial structures, either by using layer by layer growth[7], or by varying the deposition rates during growth.

The most severe problem of using evaporation techniques for in situ growth is the presence of sufficient amounts of oxygen during growth. Other fabrication techniques such as sputtering and laser-ablation can use high enough oxygen partial pressures during growth to form $YBa_2Cu_3O_y$ within the region of the pressure-temperature diagram where $YBa_2Cu_3O_y$ is thermodynamically stable according to the data of Beyers and Ahn[8]. Evaporation techniques limit the overall pressure to roughly $5x10^{-4}$ mbar, which is not sufficient. Solutions to this problem are to make locally a very high oxygen pressure near the substrate, as has been demonstrated by K.Shinohara et.al [6], or to use some form of activated oxygen, like ozone[4], or atomic oxygen[1,5,6]. The advantage of using ozone or atomic oxygen with respect to a high differential oxygen pressure is that it also allows to coat large areas and that it is easier to obtain a homogenous pressure distribution.

2. FABRICATION EQUIPMENT

The films are fabricated in a VG MBE system which consists of a growth chamber for evaporation, an analysis chamber for XPS/Auger measurements, an annealing station, and aditionally a laser ablation system. Samples can be transported from one chamber to another without breaking the vacuum. The growth chamber contains two Airco Temescal electron guns and one VG Knudsen cell. It is pumped by a turbo molcular pump and a Ti sublimation pump. Base pressure of the system is below 10^{-10} mbar. Yttrium and copper are evaporated from the e-guns and the barium is evaporated from the Knudsen cell. The filament of the Knudsen cell has been modified to deliver sufficient power at the end of the crucible to prevent condensation of material at the lip. This improves the long term drift of the barium evaporation rate from 10-20% per hour to less than 1 % per hour. The yttrium gun contains a tantalum liner to improve the stability of the melt. The evaporation flux from the electron guns is controlled by a feedback system which uses one differentially pumped mass spectrometer for each gun and a high frequency sweep for high frequency control. The bandwidth of the feedback system is larger than 100 Hz, and the long term drift is on the order of 1-2% per hour.[9] However, the sensitivity of the mass spectrometers is strongly dependent on pressure above 10^{-5} mbar. In spite of the differential pumping of the mass spectrometers this can still result in a 20-30% drift of the yttrium and copper evaporation rates during a deposition run at the highest pressure we use, because the pressure distribution in the growth chamber can change over time. The pressure dependence of the sensitivity of the mass spectrometers also limits the bandwidth of the feedback loop considerably by the gettering effect of the evaporated metals. The total pressure in the system is measured with an ionization vacuum gauge which is located near the sample holder. The fluxes from the various sources are adjusted to the desired ratios with a single quartz crystal monitor which can be moved into the sample position to provide a tooling factor of 100 %.

The ozone is produced in a commercial "silent" discharge generator.[10] This generator yields a 5% ozone/oxygen mixture at a flow rate of 50 l/h. We can produce enough ozone in 15 minutes for a deposition run of several hours. The ozone/oxygen mixture is pumped through a glass chamber which is kept at a temperature of 140 Kelvin. At this temperature mainly ozone condenses. After purification the ozone can be lead into the growth chamber through a leak valve and a stainless steel tube. The tube is directed towards the substrate to ensure that the ozone does not decompose on the chamber walls before reaching the substrate. The angle between the tube and the substrate plane is 20° and the distance between the end of the tube and the substrate is 8 centimeters. The pressure in the deposition chamber, which is proportional to the vapour pressure in the liquid ozone vessel, can be adjusted by heating the glass chamber relative to the liquid nitrogen bath. Based on geometrical and pumping speed considerations we estimate that a pressure of 1.0×10^{-4} mbar in the growth chamber corresponds to a flux of 1.5×10^{-8} mol $cm^{-2}\ s^{-1}$ of ozone on the sample position, assuming all the ozone is delivered. This flux corresponds to a partial pressure of 3.4×10^{-5} mbar. We verified the ozone flux at the sample postion with a silver coated quartz crystal[11] and estimate it to be at least 1.6×10^{-9} mol $cm^{-2}\ s^{-1}$ at a chamber pressure of 1.0×10^{-4} mbar.

The substrates are glued with silver paste to a platinum transport plate which is clamped to a tantalum block. The tantalum block is radiatively heated from the back by a 250 W quartz lamp. Because we cannot measure the temperature of the sample directly we have to deduce the temperature of the sample from the temperature of the tantalum plate. Therefore a thermocouple has been fitted in a hole in the tantalum block. The relation between the temperature of the platinum transport plate and the temperature of the tantalum block has been calibrated with a pyrometer and a thermocouple several times over a period of one year. We estimate the reproducibility of the substrate temperature measurement to be smaller than 30 °C.

3. FABRICATION PROCEDURE

The fluxes from the various sources are switched on first and are brought into their consecutive feedback loops. Then the ozone flow is turned on by heating the still. After adjustment of the ozone flow to the desired value the evaporation rates of the respective sources are set to give the desired composition. A typical total evaporation flux is 0.2 nm/s. When this calibration procedure has been completed the quartz crystal is removed and the substrate is brought into position. The tantalum block is heated to the required temperature and the shutters are opened until a film with the required thcikness is grown. The shutters are closed and sample holder is allowed to cool down in about half an hour to room temperature. The evaporation sources are switched off immediately after closing the shutters to prevent deposition of material during the cooling by scattering. During the deposition and the cool down the temperature of the ozone still is held constant, which implies that the ozone flux into the growth chamber is also constant. The sample is removed from the holder and transported to the load-lock when the temperature has dropped below 100 °C.

4. RESULTS

The results obtained on samples grown at $2x10^{-4}$ mbar and at $3x10^{-5}$ mbar chamber pressure for various temperatures are summarized in table 1. Only samples that were grown at chamber pressures of $2x10^{-4}$ mbar and with maximum purity of ozone flux are superconducting. Figure 1 shows the position of the growth conditions of the superconducting and the non-superconducting samples in the p,T diagram in combination with the extrapolated stability line for $YBa_2Cu_3O_y$ and O_2. The superconducting samples are clearly grown in the "unstable" region. The position of the superconducting and the nonsuperconducting samples in the p,T diagram is comparable to the positions found of films grown with atomic oxygen by Edwards et al.[12] The reason why the samples can be grown in the "unstable" region is still a question to be answered: either the stability line does shift due to the presence of the ozone, or the presence of ozone enhances the formation of $YBa_2Cu_3O_y$, while the decomposition of $YBa_2Cu_3O_y$ is limited by kinetics. Figure 2 shows the R(T) curves of the superconducting films. The minimum growth temperature required to obtain a superconducting film is 600 °C

Table 1. Properties of samples grown under various growth conditions.

Sample	Substrate	d [nm]	p [mbar]	ozone [%]	T [°C]	T_c [K]	XRD	c-axis [Å]
BH1a	MgO	500	$2.0x10^{-4}$	100	577	–	$YCuO_2$	–
BH1b	$SrTiO_3$+Nb[a]	500	$2.0x10^{-4}$	100	577	–	–	–
BG1	$SrTiO_3$	91	$1.8x10^{-4}$	100	599	50-4.2	–	–
BI1a	MgO	500	$1.8x10^{-4}$	100	627	80-60	poly $YBa_2Cu_3O_y$	–
BI1b	$SrTiO_3$+Nb[a]	500	$1.8x10^{-4}$	100	627	80-68	001..006 $YBa_2Cu_3O_y$	11.86
BJ1a	MgO	500	$2.9x10^{-4}$	100	652	87-47	poly $YBa_2Cu_3O_y$	–
BJ1b	$SrTiO_3$+Nb[a]	500	$2.9x10^{-4}$	100	652	88-42	poly $YBa_2Cu_3O_y$	–
BM1b	$SrTiO_3$+Nb[a]	192	$2.3x10^{-4}$	100	686	87-83	001..007 $YBa_2Cu_3O_y$	11.72
BP1a	$SrTiO_3$	239	$6.8x10^{-5}$	100	631	–	–	–
BP1b	Si	239	$6.8x10^{-5}$	100	631	–	–	–
BO1a	$SrTiO_3$	61	$3.6x10^{-5}$	100	652	–	CuO	–
BO1b	Si	61	$3.6x10^{-5}$	100	652	–	–	–
BN1	$SrTiO_3$	500	$3.0x10^{-5}$	100	672	–	$YBa_2Cu_3O_y$ (a and c axis mixed), $BaCu_2O_2$, Ba_2CuO_3, $YCuO_2$, $Y_2Cu_2O_5$ Y_2O_3, Cu_2O $YBa_3Cu_2O_y$, Y_2BaCuO_5	–
BK1	MgO	500	$2.5x10^{-4}$	5	656	–	Y_2BaCuO_5 CuO	– –
BL1a	MgO	500	$1.7x10^{-4}$	5	646	–	$BaCu_2O_2$	–
BL1b	$SrTiO_3$+Nb[a]	500	$1.7x10^{-4}$	5	646	–	$BaCu_2O_2$	–
BE1	$SrTiO_3$	200	$>4.0x10^{-4}$	0	661	–	–	–

a) Some of the $SrTiO_3$ substrates were doped with 200 ppm Nb.

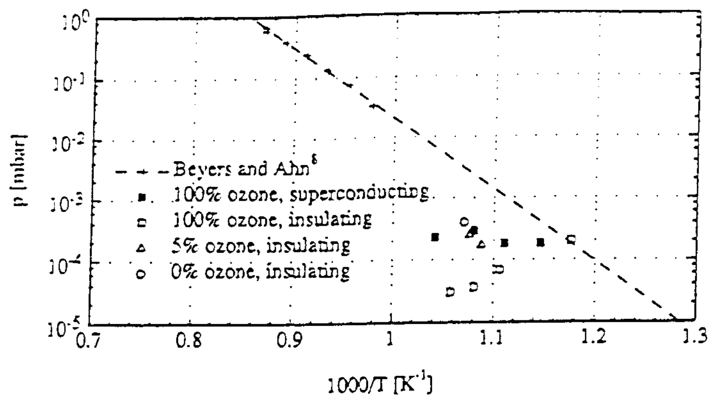

Figure 1. Position of the samples listed in table 1 in the pressure versus inverse temperature diagram as compared to the extrapolation of the stability line of Beyers and Ahn.[8]

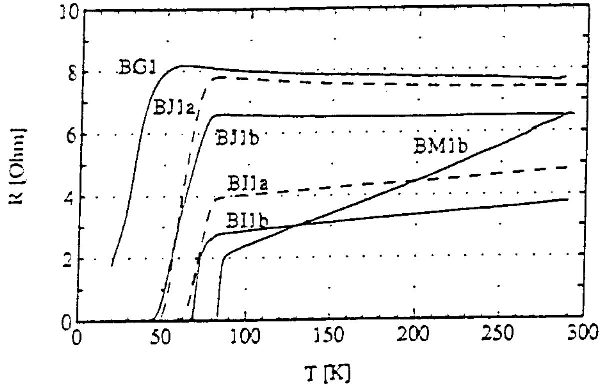

Figure 2. Resistance vs. temperature of the superconducting samples listed in table 1.

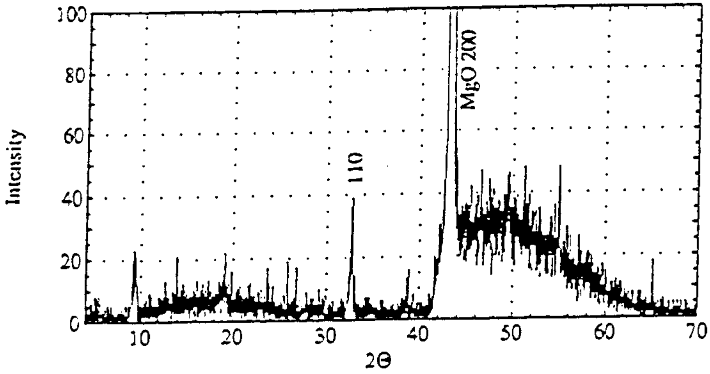

Figure 3. XRD scan of sample BJ1a. The scan shows only the (110) peak of $YBa_2Cu_3O_y$ and the MgO 200 peak, indicating that the sample is polycrystalline. The sample was grown at a temperature of 652 °C and a pressure of 2.9×10^{-4} mbar, using the maximum purity ozone flux. The sample has a transition of 87-47 K.

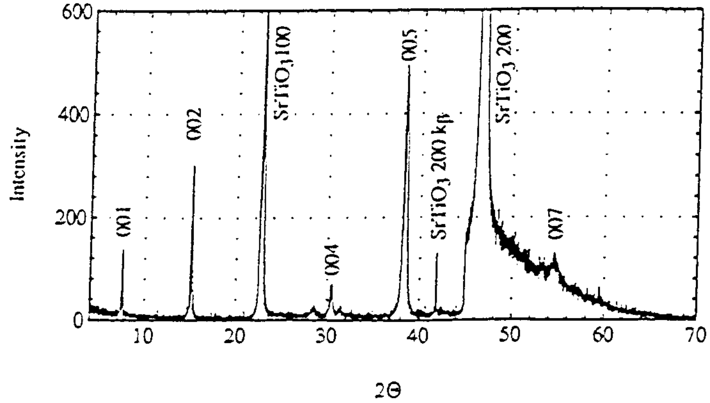

Figure 4. XRD scan of sample BM1b. This sample is predominantly c-axis oriented. It was grown at a temperature of 686 °C and a pressure of 2.3×10^{-4} mbar, using the maximum purity ozone flux. The sample has a transition of 87-83 K.

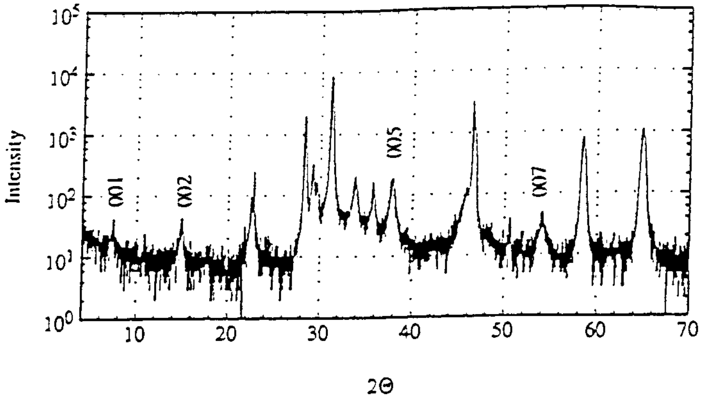

Figure 5. XRD scan of the non superconducting sample BN1. The strongest peaks can be assigned to $YCuO_2$ (or $YBa_3Cu_2O_y$), Ba_2CuO_3, $BaCu_2O_2$, and $YCuO_2$ (or Y_2BaCuO_5). Note that a small amount of $YBa_2Cu_3O_y$ is also present. The sample was grown at a temperature of 672 °C and a pressure of 3.0×10^{-5} mbar, using the maximum purity ozone flux.

(sample BG1). Figure 3 shows the XRD scan a sample BJ1a which was grown at 652 °C. This scan shows only the 110 peak of $YBa_2Cu_3O_y$, which indicates that the film is polycrystalline. A well oriented film with a linear R,T behaviour (like sample BM1b) requires a growth temperature of at least 680 °C. Figure 4 shows the XRD scan of sample BM1b: this sample is predominantly c-axis oriented. A 400 °C post anneal in ambient oxygen did not change the R(T) curve of this sample, indicating that the sample is fully loaded with oxygen during the cooling in the evaporator.

Table 1 also contains data on samples grown with a 5 % ozone/oxygen mixture (i.e. directly from the generator) or with pure oxygen at conditions comparable to the growth conditions of the superconducting samples. None of these samples are superconducting. Figure 5 shows a XRD scan of one of the non-superconducting samples, BN1, which was grown at 672°C and at $3x10^{-5}$ mbar. The strongest XRD peaks can be assigned to $YCuO_2$ (or $YBa_3Cu_2O_y$), Ba_2CuO_3, $BaCu_2O_2$, and $YCuO_2$ (or Y_2BaCuO_5). Note that a small amount of $YBa_2Cu_3O_y$ is also present.

5. CONCLUSIONS

We have grown in situ superconducting $YBa_2Cu_3O_y$ films by reactive coevaporation at low pressures using ozone. The films are grown below the extrapolated $YBa_2Cu_3O_y$ stability line for oxygen. The minimum temperature to grow a superconducting film at a chamber pressure of $1.8x10^{-4}$ mbar and maximum purity ozone flux was determined to be 600 °C. The growth of a well crystallized c-axis oriented film with a $T_{c,0}$ of 83 K requires a temperature of at least 680 °C at a pressure of $2.3x10^{-4}$ mbar and maximum purity ozone flux. Superconducting films grown at lower temperatures are polycrystalline according to XRD scans. Films grown in the temperature region 631-672 °C and at pressures below 10^{-4} mbar with maximum purity ozone flux (or with low purity ozone flux at $2x10^{-4}$ mbar) are not superconducting.

6. REFERENCES

1 R.M.Silver, A.B.Berezin, M.Wendman, and A.L.de Lozanne, Appl.Phys.Lett 52, 2174 (1989).

2 C.B.Eom, J.Z.Sun, K.Yamamoto, A.F.Marshall, K.E.Luther, T.H.Geballe, and S.S.Laderman, Appl. Phys. Lett. 55, 595 (1989).

3 T. Venkatesan, X.D.Wu, B.Dutta, A.Inam, M.S.Hegde, D.M.Hwang, C.C.Chang, L.Nazar, and B.Wilkens, Appl. Phys. Lett. 54, 581 (1989).

4 D.D.Berkley, B.R.Johnson, N.Anand, K.M.Beauchamp, L.E.Conroy, A.M.Goldman, J.Maps, K.Mauersberger, M.L.Mecartney, J.Morton, M.Tuominen, and Y-J.Zhang, Appl. Phys. Lett. 53, 1973 (1988).

5 N.G.Chew, S.W.Goodyear, J.A.Edwards, J.S.Satchell, S.E.Blenkinsop, and R.G.Humphreys, Appl.Phys.Lett. 57, 2016 (1990).

6 K.Shinohara, V.Matijasevic, P.A.Rosenthal, A.F.Marshall, R.H.Hammond, and M.R.Beasley, Appl.Phys.Lett.58, 756 (1991).

7 D.G.Schlom, A.F.Marshall, J.T.Sizemore, Z.J.Chen, J.N.Eckstein, I.Bozovic, K.E.von Dessonneck, J.S.Harris jr., and J.C.Bravman, submitted to Journal of Crystal Growth.

8 R.Beyers, and B.T.Ahn, to appear in Annual Review of Materials Science, Vol.21, (1991).

9 H.M.Appelboom, P.Hadley, D.van der Marel, and J.E.Mooij, IEEE Trans. Magn. Vol.27, No.2, 1467 (1991).

10 M.Horváth, L.Bilitzky, and L.Hüttner, Ozone (Elsevier Science Publishers, Amsterdam , 1985).

11 V.Matijasevic, E.L.Garwin, and R.H.Hammond, Rev.Sci.Instrum. 61, 1747 (1990).

12 J.A.Edwards, N.G.Chew, S.W.Goodyear, J.S.Satchell, S.E.Blenkinsop, and R.G.Humphreys, J.Less Comm. Mat.164&165, 414 (1990).